Pergamon
www.elsevier.com/locate/asr
Available online at www.sciencedirect.com
SCIENCE DIRECT®
doi: 10.1016/S0273-1177(03)00828-7

DEVELOPMENT OF THE GRAVITY PROBE B FLIGHT MISSION

J. P. Turneaure[1], C. W. F. Everitt[1], B. W. Parkinson[1], D. Bardas[1], S. Buchman[1], D. B. DeBra[1], H. Dougherty[2], D. Gill[1], J. Grammer[3], G. B. Green[4], G. M. Gutt[1], D.-H. Gwo[1], M. Heifetz[1], N. J. Kasdin[4], G. M. Keiser[1], J. A. Lipa[1], J. M. Lockhart[1,5], J. C. Mester[1], Barry Muhlfelder[1], R. Parmley[3], A. S. Silbergleit[4], M. T. Sullivan[1], M. A. Taber[1], R. A. Van Patten[1], R. Vassar[3], S. Wang[1], Y. M. Xiao[1], and P. Zhou[1]

[1]*W. W. Hansen Experimental Physics Laboratory, Stanford University, Stanford, CA 94305, USA*
[2]*Space Systems Division, Lockheed Martin Missiles and Space, 2690 Hanover St., Palo Alto, CA, 94304, USA*
[3]*Advanced Technology Center, Lockheed Martin Missiles and Space, 3251 Hanover St., Palo Alto, CA, 94304, USA*
[4]*NavAstro, 204 More Avenue, Los Gatos, CA 95030, USA*
[5]*Department of Physics and Astronomy, San Francisco State University, 1600 Holloway Avenue, San Francisco, CA, 94132, USA*

ABSTRACT

Gravity Probe B is an experiment to measure the geodetic and frame-dragging precessions, relative to the "fixed" stars", of a gyroscope placed in a 650 km altitude polar orbit about the earth. For Einstein's general relativity, the precessions are calculated to be 6.6 arcsec/yr for the geodetic precession and 0.042 arcsec/yr for the frame-dragging precession. The goal of the experiment is to measure these precessions to better than 0.01% and 1%, respectively. This paper gives an overview of the experiment and a discussion of the flight hardware development and its status. This paper also includes an estimate of the geodetic and frame-dragging errors expected for the experiment.

INTRODUCTION

The idea of testing general relativity with orbiting gyroscopes was advanced just over 36 years ago independently by L. I. Schiff (1960) and G. E. Pugh (1959). According to Schiff's calculation, a gyroscope in a 650 km altitude polar orbit about the earth will experience two relativistic effects acting at right angles: (1) a geodetic precession of 6.6 arcsec/yr in the plane of the orbit due to Fermi-Walker transport about the earth, and (2) a frame-dragging precession of 0.042 arcsec/yr at right angles to the orbit plane due to the earth's rotation. These effects are measured with respect to the fixed stars. The goal of the Gravity Probe B (GP-B) is to measure them to better than 0.01% and 1%, respectively.

Although much progress has been made in testing general relativity, particularly since about 1960 when Pound and Rebka (1960) reported the first accurate (5%) observations of the gravitational redshift, the most accurate non-null tests of general relativity have been stuck since 1977 at about 0.1% when Shapiro (1977) reported measurements of the Shapiro time delay due to passage of a microwave signal through the sun's gravitational potential using the transponder on the Mars' lander. Measurements of the deflection of starlight (Lebach *et al.*, 1995) and the de Sitter precession of the earth-moon system in the gravitational potential of the sun (Chandler *et al.*, 1995) have also reached about the 0.1% level. It should be noted that the gravitational redshift has been measured with an accuracy of about 0.01% in Gravity Probe A (Vessot and Levine, 1977), but this test is a confirmation of the equivalence principle, rather than a consequence of general relativity. The book by Will (1993) gives an extensive treatment of the testing of general relativity. The article by Keiser (2003) treats the testing of general relativity in space. We expect GP-B's measurement of the geodetic effect, which is related to the de Sitter effect, to improve the accuracy of non-null tests of general relativity by a factor of from 10 to 50. Also, the measurement of the frame-dragging

Adv. Space Res. Vol. 32, No. 7, pp. 1387–1396, 2003

Printed in Great Britain
0273-1177/$30.00 + 0.00

effect will be the first direct measurement of this phenomena, which is due to the dragging of space-time by the rotation of a massive body.

NASA funding for the GP-B commenced in November 1963, with funding for development of the flight system beginning in March 1985. The papers by Everitt (1988), Turneaure *et al.* (1985), and Bardas *et al.* (1986) give overviews of the program through about 1986. The effort since 1985 can be divided into three phases: The first phase consists of refining and completing the development of the science instrument technology and undertaking a program of "incremental prototyping" of the full-size science payload. The second phase consists of the final design, fabrication, assembly, integration, and verification of the flight system. The third phase consists of launch and operation of the space vehicle, followed by analysis of the science data. The space vehicle comprises the payload, which contains the science instrument, and the spacecraft, which provides the more standard support features for the payload. The first of these phases is nearly complete with the only major remaining activity being the completion of the GTU-2 test, which is the fourth full-size payload system test and is part of our "incremental prototyping" approach to the payload. We are well into the second phase. The flight payload design is nearly complete and well into fabrication, assembly and test. The spacecraft is also well into design with several subsystems in fabrication. Planning for the third phase is in progress.

"Incremental prototyping" has been an essential feature of our science payload development. Although the principles employed for the science instrument assembly were in most cases well established in 1985, the engineering heritage for the integrated instrument still had to be developed. This also applied to the vacuum probe, which is complex and has many features unique to GP-B. At the start of our flight development in 1985, there was some engineering and flight heritage for superfluid helium dewars from the IRAS (Infrared Astronomy Satellite) and the COBE (Cosmic Background Explorer) programs. However, there was no flight heritage for some of the dewar design features needed by GP-B due to its ultralow magnetic field requirements. We have used "incremental prototyping" to establish the needed engineering heritage for all aspects: design, fabrication, assembly, integration, and test. In our "incremental prototyping" approach, we have attacked the hardest engineering problems first while still using full-size flight prototypical designs with flight interfaces, but with reduced functionality and without costly flight build standards. We have completed three full-size payload system tests (FIST, GTU-0, GTU-1) and are in the final preparation for the last in our "incremental prototyping" series (GTU-2). "Incremental prototyping" has allowed us to smoothly and confidently proceed to our flight design.

EXPERIMENT DESCRIPTION AND STATUS

The essence of the experiment is to accurately measure the precession of a gyroscope relative to the fixed stars with one star whose proper motion is accurately known chosen as the guide star. A gyroscope is placed in a drag-free polar orbit with an ascending node so the line of sight to the guide star lies in the orbit plane. The gyroscope is spun up so its axis is pointed toward the guide star. The selection of the guide star, which is baselined as HR5110, is discussed by Gwo *et al.* (2003). Note that the predicted frame-dragging precession is reduced by the cosine of the guide star's declination, whereas the geodetic precession is unaffected. Since the declination of HR5110 is about 37 deg north, the predicted frame-dragging precession is 34 marcsec/yr. For a polar orbit the two relativity precessions are orthogonal to one another: the geodetic precession is about the orbit normal and the frame-dragging precession is about the earth's rotation axis. The gyro precession angle is read out by employing a telescope actively pointed at the guide star and mechanically coupling the gyro pick-up loop, located on the gyro housing, to the telescope. Thus, since the telescope is pointed at the guide star, the gyro readout signal is a measure of the gyro precession angle relative to the guide star. The gyro readout scale factor is precisely calibrated during the experiment using the aberration of starlight due to the motion around the earth and the sun. Since the aberration signal is largely uncorrelated with other expected signals, the scale factor can be precisely extracted in data analysis. Two additional features discussed below enhance the experiment: a slow roll about the line of sight to the guide star with a period between 1 and 3 minutes, and low temperature operation at about 2.5 K.

The four gyroscopes are aligned with the guide star, two spinning clockwise and two counter clockwise. They are all mounted in a line on the space vehicle roll axis. One serves as the drag-free sensor and thus has a mean acceleration acting on it very close to zero. The other three are subject to gravity gradient accelerations having values up to about 10^{-7} g. But because of the configuration, the dc component of this acceleration is parallel to the

gyro spin axis and produces negligible cross-track acceleration. Thus the mass unbalance torque on all four gyroscopes is reduced by a factor of 10^{-12} below that expected for operation of the gyroscopes in 1 g.

Roll. Roll about the line of sight to the guide star provides four essential features. (1) Roll greatly reduces the effects of bias drifts on the precession measurements since it places the signal at roll frequency. Examples of bias drifts include (a) drifts in the orientation between the telescope and gyro readouts due to structural creep, relaxation and thermal expansion, and (b) electronic bias drifts in the gyro and telescope readouts. (2) Roll reduces the gyro and telescope readout noise by translating their signals to the roll frequency, away from dc where noise is greatly enhanced by a 1/f (or worse) power spectrum. (3) Roll averages the largest disturbance torques that are fixed to the body of the gyro housing: the averaging factor is 5×10^{-5} assuming the required time-averaged angle between the gyroscope and the guide star of 10 arcsec. (4) Roll allows a single gyro pick-up loop and its readout to measure both the geodetic and frame-dragging precessions. The signal amplitude is a measure of the total precession angle, and the signal phase is a measure of the amplitude split between the geodetic and frame-dragging directions.

Low-Temperature. For our experimental approach, low temperature provides two essential features. (1) At low temperature, the small thermal expansion coefficient of fused quartz as well as the high degree of thermal isolation from the space environment reduces the thermal bending at roll frequency between the telescope and gyro readouts, which could masquerade as a precession signal, to a negligible level. (2) The low temperature environment also allows the experiment to use a superconducting magnetic gyro readout system utilizing the London magnetic dipole moment of a spinning superconductor (the gyro rotor), the ultralow noise magnetic readout of a dc SQUID (without significantly disturbing the gyroscope), and the very precise temperature control required for the dc SQUID.

Science Instrument Assembly

The Science Instrument Assembly (SIA), which is partially illustrated in Figure 1, comprises four gyroscopes, a drag-free proof mass, and a star tracking telescope all held together with a fused-quartz block, and four dc SQUID packages for the gyro readout. The SQUID packages are mounted on the probe and not shown in the figure. The gyroscopes are installed in the fused-quartz block so their centers are within 0.1 mm of a line parallel to the telescope axis. This alignment is required to reduce the centripetal acceleration on the gyroscopes due to the roll of the space vehicle. The SIA is maintained at about 2.5 K using the vacuum probe and dewar described later. Each gyroscope independently measures the geodetic and frame-dragging precessions thus giving both measurement and failure redundancy. Using the star tracking telescope as a sensor, the entire space vehicle, as well as the SIA, slowly rolls about the line of sight to the guide star. During science data taking, the GP-B space vehicle uses Gyro #1 as the drag-free sensor for drag compensation of the space vehicle. Gyro #2 and the drag-free proof mass are available as backups. We have completed three integrated payload system tests with incremental improvements to the SIA. For the next test (GTU-2), we plan to include a telescope for the first time.

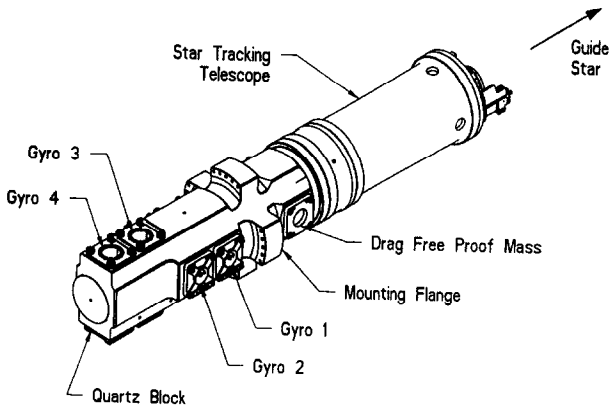

Fig. 1. Isometric view of science instrument assembly, which is about 1.1 m in length.

Gyroscope. An exploded view of the gyroscope is shown in Figure 2. The gyro rotor consists of a spherical fused-quartz or single-crystal silicon ball 38.1 mm in diameter coated with a uniform 1.25 μm layer of Nb. The rotor is placed inside of a fused-quartz housing composed of two halves: a readout half and a spin-up half. The gyro housing has six electrodes forming three mutually orthogonal pairs. The coating and characteristics of these 7-layer 2.5 μm thick Ti-Cu electrodes are described by Zhou *et al.* (1995). A 3-phase 70 kHz signal is applied to the electrodes to capacitively measure the vector position of the rotor relative to the electrodes. Using this position information, either dc or low frequency voltages are applied to the electrodes to force the rotor to the housing

center. The forcing voltages vary between about 600 V when suspending the gyro rotor on the ground in 1 g and about 0.1 V when suspending the gyro rotor on orbit. There are a number of support pads, which prevent the rotor from coming into contact with the electrodes and which provide a three-point support for mechanically caging the gyro rotor during launch to prevent it from rattling. The pads and the remaining interior of the gyro housing are covered with a 0.12 μm thick Ti layer to act as a Faraday shield against charges that will be trapped in the fused quartz due to particle radiation on orbit.

The spin-up half of the gyro housing contains a channel for helium gas spin up of the gyro rotor. The gas is injected into the channel at nearly the speed of sound through a nozzle and is pumped through an exhaust line at the output of the channel. A 14 μm thick layer of Ti-Cu-Ti is placed around the spin-up channel to control leakage of gas out of the channel. The optimization of the spin-up channel and the nozzle is the last major improvement made in the gyro design. Experiments have shown that the optimal channel depth for reaching the greatest asymptotic spin speed is 0.27 mm. Also, improvements have been made in the precision with which the nozzle is installed so that the gas flow is optimally directed into the channel. With these improvements, an asymptotic spin speed of 214 Hz has been demonstrated using ^{3}He gas at 6.5 K. Since each gyroscope is spun up in turn, the other three gyroscopes will spin down due to drag from the leakage gas while the current one is being spun up. In practice, we expect to be able to reach approximately 80% of the asymptotic spin speed for the four gyroscopes. After fine adjustment of the initial spin direction by torquing the gyroscope using its quadrupole shape and modulation of the electrode voltages at roll, the spin axis will be aligned to within 10 arcsec of the line of sight to the guide star (Bencze, 1996).

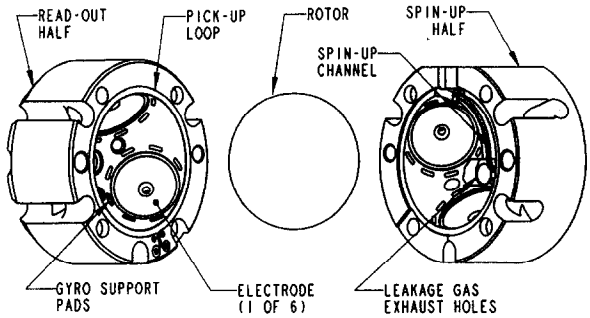

Fig. 2. Exploded view of the gyro rotor and its housing.

The gyroscope has undergone a long evolutionary design history, starting in the 1960s, with the design of the first flight prototypes begun in 1984. They have been used in our payload system tests since 1988 and have undergone over 90,000 hr of suspended operation. The flight gyroscopes are now in manufacture with 6 bare gyro rotors (3 fused-quartz and 3 single-crystal silicon) and 6 bare gyro housings delivered for coating. The manufacturing methods have been fully developed and meet our flight requirements.

Gyro Readout. Figure 3 is a schematic of the gyro readout. The spinning gyro rotor, whose niobium coating is superconducting below about 9 K, produces a magnetic dipole moment, called the London moment. For a gyro rotor spinning at 140 Hz, the London magnetic field, B_L, is 1.0×10^{-8} T. A 4-turn superconducting Nb thin film pick-up loop, which is schematically shown in Figure 2, is wound on the read-out housing half around the gyro rotor. The pick-up loop is connected through a low inductance superconducting stripline cable to the input of a dc SQUID, which converts the magnetic flux through the pick-up loop to a voltage signal at its output. Since initially the rotor spin vector and thus the magnetic dipole vector is nearly in the plane of the pick-up loop, the output signal is also nearly zero. As the gyro rotor precesses away from the plane of the pick-up loop, the flux through the pick-up loop increases producing a signal at the output of the dc SQUID electronics. Since the SIA rolls about the line of sight to the guide star and the pick-up loop is fixed to the gyro housing (also rolling), the signal is modulated at the roll frequency away from dc where 1/f noise is large. Recent end-to-end gyro readout experiments in GTU-1 have demonstrated a single-sided noise of 190 marcsec/$\sqrt{\text{Hz}}$ (assuming a 130 Hz spin speed and a 3 minute roll period), which meets the experiment

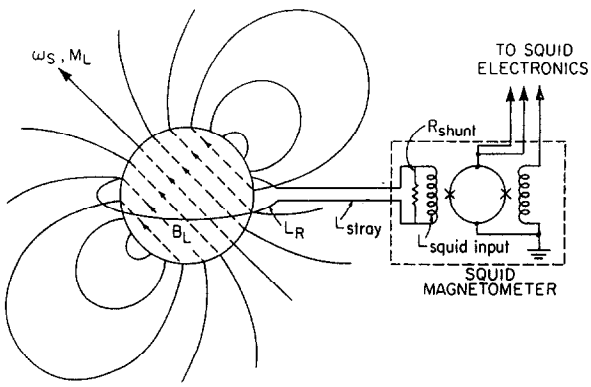

Fig. 3. Simplified schematic of gyro readout system.

requirement. Flight prototype gyro readout hardware is being assembled now for use in GTU-2. Muhlfelder *et al.* (2003) give a more complete discussion of the gyro readout development and performance.

A high performance magnetic shielding system and a magnetics properties control program are required for proper operation of the gyro readout system: the attenuation of external magnetic field variations is required to be greater than 10^{12} and the residual magnetic field at the gyro locations is required to be less than 10^{-10} T. These requirements are met by a magnetic shielding system and rigid magnetics screening of materials and parts used in magnetically sensitive regions of the payload. The magnetic shielding system is described by Lockhart (1986).

Telescope. Figure 4 is a schematic of the cryogenic fused-quartz star tracking telescope, which has an aperture of 144 mm and an overall length of 505 mm. The telescope is a modified Cassegrainian system, which utilizes three spherical mirrors and a Schmidt corrector arranged so that the focal position is in front of the corrector. For the flight telescope, the spherical optics are actually expected to be compensated with an elliptic correction to the primary mirror. An image dividing assembly splits the photon beam into two diffraction limited images, which fall onto a sharp roof-edge prism, one for each readout axis. When the image falls onto the center of the roof prism, the image is divided into two equal photon beams which are then transported to and read out with Si PIN diodes and Si JFET amplifiers. The linearity, linear range, and angle equivalent noise are all expected, based on sub-system tests, to meet our requirements. The telescope design, manufacturing, and verification are discussed by Gwo *et al.* (2003).

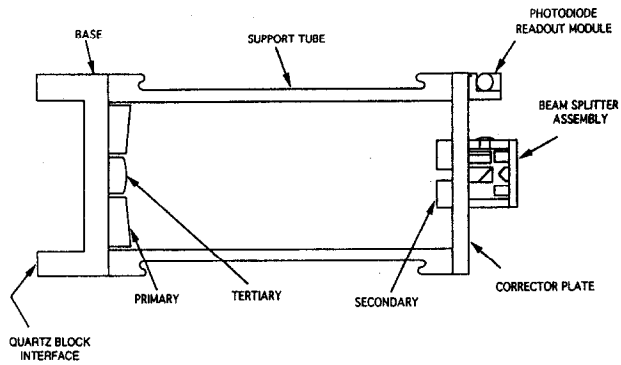

Fig. 4. Cryogenic fused-quartz star tracking telescope.

Payload

Figure 5 is a cut-away view of the GP-B payload showing the SIA, the probe and the dewar. Not shown in the figure are the sunshade, the payload electronics, and the cross flange. The sunshade, which is shown in Figure 6, prevents light from the sun and other bright sources from reaching the cryogenic star tracking telescope for cone angles greater than 18 deg. The payload electronics is partitioned into a forward region and an aft region. The sensitive low-level electronics are placed in the forward region near the probe electrical connectors, and they are enclosed with a cover that passively reduces the peak-to-peak variations in electronics box temperatures to ≤ 30 mK at roll frequency. The cross flange, which is mounted on top of the probe, has two valves for pumping out the probe and a sapphire window through which the telescope can view the guide star. As part of our "incremental prototyping" approach, three integrated system payload development tests have been completed and one more is planned before the final integration and test of the payload (Taber, 1994, 2003).

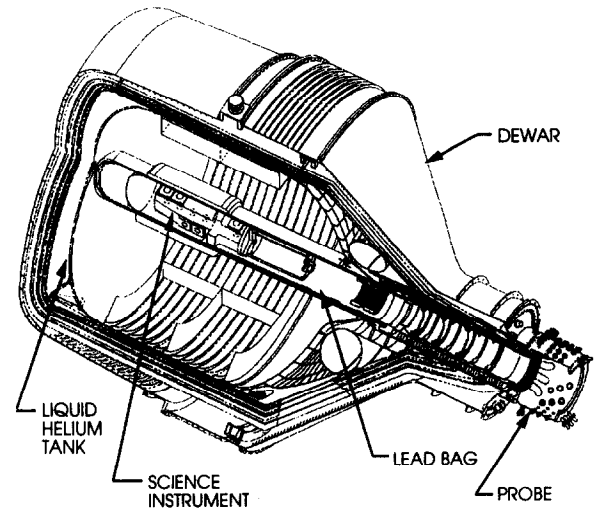

Fig. 5. Cutaway view of GP-B payload. The dewar is 2.2 m in diameter.

Probe. The probe, which houses the SIA, provides the required ultrahigh vacuum, ultralow magnetic field, and very clean (low levels of particulate contamination) environment; plumbing lines for gyro spin up and for gyro caging; and the many electrical cables for operation of the instrument. The probe is our most complex mechanical assembly. For this reason, we planned to sequentially design and build three probe models (Probe A, B, and C) in

our "incremental prototyping" approach to provide us with the heritage needed for the design and build of the flight probe. Probe A was used in the first two integrated payload system tests (FIST and GTU-0). Probe B, which was designed and built to flight standards so that it could be used as a flight backup after refurbishment, was used in the third integrated payload system test (GTU-1) and is also being used in the fourth integrated payload system test (GTU-2). Probe C, the flight probe, is currently being assembled.

Dewar. The flight dewar contains 2319 l of superfluid liquid helium at launch, and it is estimated to have a minimum on-orbit lifetime of 17.3 month. Integral to the dewar (located just outside of the probe) is a Cryoperm® magnetic shield and a superconducting lead bag, which provide a magnetic field in the region of the gyroscopes of 10^{-11} T. In our first three payload system tests (FIST through GTU-1), we used a simplified lab dewar, called the Engineering Development Dewar (EDD). The EDD with its flight interfaces to the probe and its flight prototypical magnetic shield and lead bag allowed us to design and verify these specialized features using our "incremental prototyping" approach before embarking on the final design of the flight dewar. The flight Science Mission Dewar (SMD) has been assembled and is now undergoing verification testing. The SMD will also be verified in the GTU-2 testing.

Space Vehicle

Figure 6 illustrates the GP-B space vehicle. It is separated into the payload, described above, and the spacecraft, which provides the rest of the space vehicle sub-systems. The spacecraft includes a number of features: (1) a set of proportional thrusters utilizing the boil-off gas from the helium dewar to control the space vehicle attitude and roll, and to maintain a pure gravitational orbit using Gyro #1 as an isolated, undisturbed drag-free sensor; (2) a set of mass trim mechanisms for on-orbit fine adjustment of the mass properties to place the space vehicle center of mass close to the roll axis and to set two of the cross products of inertia close to zero (keeps the control authority for the drag-free and roll control system within its capability); (3) two star trackers to sense the roll angle of the space vehicle, as well as pitch and yaw; (4) a set of Global Positioning System (GPS) antennas and a GPS receiver to accurately and autonomously determine the space vehicle orbital parameters; (5) a set of omnidirectional antennas for communication; (6) four solar GaAs array panels for powering the space vehicle, and (7) the needed electronics. The integrated space vehicle will have a mass of about 3000 kg.

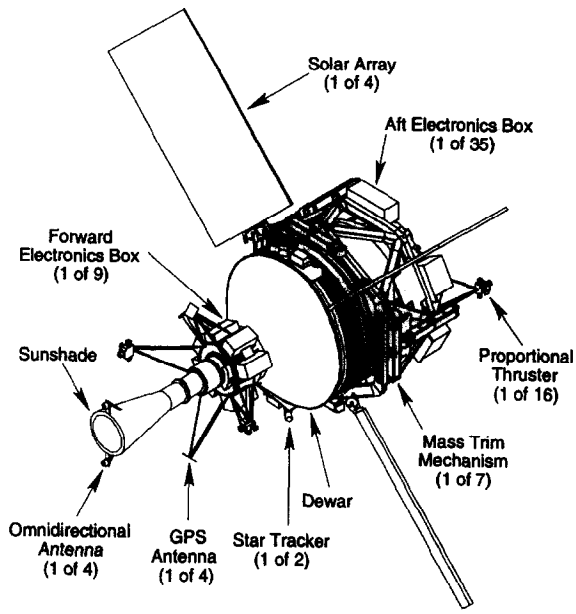

Fig. 6. Isometric view of the space vehicle. Its overall length is about 5.8 m.

Launch and On-Orbit Operations

The launch of the space vehicle into its 650 km altitude polar orbit will be aboard a two-stage Delta II launch vehicle from the Western Test Range at Vandenberg Air Force Base. The orbit inclination and ascending node are required to be very precise to achieve low gyro disturbance torques, separate the geodetic and frame-dragging precessions, and simplify the data analysis. The inclination is set to 90 deg ± 0.7 arcsec, and the accuracy of the ascending node is set to be within ± 7 arcsec of the target, which is approximately equal to the right ascension of the guide star. The orbit eccentricity is set to 0.0013 with the perigee directed toward the north, which yields a stable eccentricity (Axelrad, 1990). These precise orbital parameters are achieved through a combination of initial injection by the Delta II launch vehicle and trimming of the orbit using the proportional thruster control system and the helium dewar boil-off gas during the first 40 days of on-orbit operations. An on-board GPS receiver provides precise real-time measurement of the orbital parameters during orbit trim, as well as throughout the mission. The first 40 days will also be used for on-orbit pre-calibration of the instrument and experiment initialization. The

primary science data taking period will occur over at least 13 months depending on the dewar lifetime. Finally, there will be a period of about 2 months of post-calibration, which will be used for further detailed calibration of the instrument to allow removal of gyro precession due to the largest disturbance torques and to increase the confidence in the experiment outcome.

ESTIMATED EXPERIMENT ERROR

The GP-B experiment error, for the experimental configuration described above, was first estimated in the late 1970s (Everitt *et al.*, 1980). This was followed by a series of Ph.D. dissertations, which were studies of the data reduction process and the resulting data reduction error due to measurement noise and other experimental noise processes (the first by Vassar (1982) and the most recent by Haupt (1996)). This work has been used to guide the development of the experiment hardware. The error discussion can be divided into three areas: the uncertainty in the proper motion of the guide star, the uncertainty in the gyro precession due to classical disturbance torques, and the data reduction error.

Uncertainty in the Proper Motion of Guide Star

The current baseline guide star is HR5110, which has a visual magnitude of 5.0, a right ascension of 13:34:48, and a declination of 37.183 deg north. Ratner and Shapiro (1995) has estimated the uncertainty in the proper motion using the current available data plus two additional VLBI measurement epochs per year until the GP-B mission ends (~ 2001). The uncertainty is estimated for two cases. First, assuming the proper acceleration is fixed, the uncertainty is expected to be between 0.03 marcsec/yr and 0.06 marcsec/yr. Second, assuming that the proper acceleration must be estimated, the uncertainty is expected to between 0.08 marcsec/yr and 0.2 marcsec/yr. We do not expect the uncertainty in the proper motion to be a limiting factor in the experiment error. If for some unexpected reason the uncertainty in the proper motion of the guide star is a significant portion of the experiment error at the end of the GP-B mission, it can be reduced by continuing proper motion measurements for several additional years.

Uncertainty in the Gyro Precession due to Classical Disturbance Torques

The dominating classical disturbance torques are expected to be due to the electric fields required to support three of the four gyroscopes in the center of their gyro housings because of the gravity gradient and a small centripetal acceleration. Although the remaining gyroscope acts as a drag-free sensor, it still requires small electric fields to sense its position relative to its housing and to measure its electric charge, and thus this gyroscope is also subject to the electric field dependent disturbance torques (although substantially smaller). There are also electric field independent disturbance torques, such as differential gas damping, acting on the gyroscopes, but they are generally smaller. Here we give worst case estimates of the disturbance precessions for the gyroscope furthest from the drag-free sensor assuming a spin speed of 140 Hz. The worst case, uncompensated drift rates are estimated to be 0.20 marcsec/yr in the EW direction and 0.13 marcsec/yr in the NS direction. The frame-dragging precession is in the EW direction and the geodetic precession is in the NS direction. In-flight calibration (Everitt, 1988) allows us to measure the parameters needed to estimate some of the actual gyro disturbance torques and to remove the resulting precession from the uncompensated precession. We expect this is easily done for the two largest disturbance torques in the EW direction. After compensation for these two disturbance torques, the worst case uncertainty in both directions is 0.13 marcsec/yr. There is the possibility of measuring additional parameters during the in-flight calibration and further reducing the uncertainty in the classical gyro precession.

Data Reduction Error

The frame-dragging and geodetic precession coefficients and their standard errors, as well as those for others such as the bending of starlight, are extracted in the data reduction process. The data reduction error depends both on the data reduction model and algorithm, and on the experimental performance parameters. Table 1 gives a list of the key experimental performance parameters and provides values from several perspectives labeled as "1σ", "3σ", "90% likelihood", and "design criteria". The 1σ and 3σ values are based on our current design and test knowledge of the hardware and on the rough assumption that a normal distribution describes the likelihood of achieving a

particular value with the 1σ and 3σ values having 84% and 99.86% likelihoods of being equaled or exceeded. The second unlabeled column in the table indicates whether it is more favorable for the parameter to be larger or smaller.

Table 1. Key Experimental Parameters Affecting the Data Reduction Error

Parameter		1σ	3σ	90% Likelihood	Design Criteria
Experiment Duration (month)	≥	14	13	13	13
Roll Period (min)	≤	2	3	2.35	2
Readout Noise (marcsec/√Hz)	≤	190	250	215	190
Spin Speed (Hz)	≥	150	130	140	140
Duty Factor	≥	0.48	0.44	0.44	0.44
Calibration Signal Stability (%/yr)	≤	0.0015	0.0025	0.0025	0.0010
Scale Factor Stability (%/yr)	≤	0.03	0.05	0.05	0.05
Roll Phase Stability (arcsec/yr)	≤	6	10	10	10
Nonlinearity (%)	≤	0.006	0.012	0.012	0.010

We estimate the data reduction error using simulated science data for two different parameter sets from Table 1. In the first case, we use the set labeled "90% likelihood". These values are found by approximately minimizing the data reduction error while constraining the parameter values so they have a collective 90% likelihood of being met. The collective likelihood is the multiplication of the likelihoods of the individual parameters. They give data reduction errors (1σ) of 0.30 marcsec/yr for both the frame-dragging and the geodetic precessions. In the second case, we use the set labeled "design criteria". It is our judgment that with additional, but feasible, effort these "design criteria" can be achieved with high likelihood. The "design criteria" set gives the data reduction errors plotted in Figure 7 as a function of experiment duration. For a 13 month experiment duration, the frame dragging and the geodetic precessions are 0.20 marcsec/yr and 0.24 marcsec/yr, respectively.

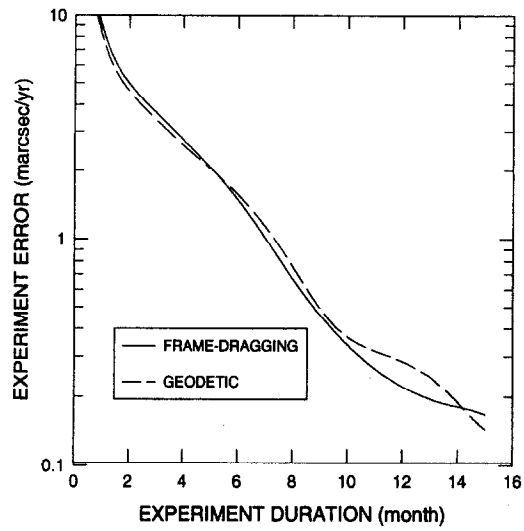

Fig. 7. Data reduction error for a single gyroscope as a function of experiment duration using the "design criteria" parameters given in Table 1.

Experiment Error Summary

The experiment standard error is the root-sum-square of the three error sources described above since they are expected to be statistically independent. For the reasons discussed above, the uncertainty in the proper motion is expected to have a negligible contribution to the experiment error. Combining the data reduction error for the "design criteria" parameter values and the worst case uncertainty in the classical gyro precession yields experiment standard errors of 0.24 marcsec/yr for the frame-dragging precession and 0.27 marcsec/yr for the geodetic precession. If all four gyroscopes give consistent results, the gyroscope ensemble is likely to yield an overall experiment error of 0.12 marcsec/yr for the frame-dragging precession and 0.14 marcsec/yr for the geodetic precession.

CONCLUSIONS

The Gravity Probe B experiment is nearly at the end of its "incremental prototyping" effort and is well into the build of the flight space vehicle. We have completed three of the four integrated payload system tests that are part of our "incremental prototyping" approach. The remaining test, GTU-2, is in preparation and will be completed in 1997. The design, fabrication, assembly and test of the flight payload sub-systems are in an advanced state with the flight dewar expected to be delivered in 1996 and the complete flight payload projected to be delivered for space vehicle integration in 2001. We expect the launch of the space vehicle in 2003 followed by about 17 months of on-orbit operations. The experiment standard errors for a single gyroscope are estimated to be 0.24 marcsec/yr for the frame-dragging precession and 0.27 marcsec/yr for the geodetic precession, which yield measurements of the predicted effects to 0.7% and 0.004%, respectively. If all four gyroscopes give consistent results and are combined, experiment errors of half these values are possible.

ACKNOWLEDGMENTS

We wish to thank the GP-B team, consisting of both staff and students at Stanford University and Lockheed Martin Missiles and Space, for their dedicated efforts. This work has been supported by NASA contract NAS8-39225 from the George C. Marshall Space Flight Center.

REFERENCES

Axelrad, P., A Closed Loop GPS Based Orbit Trim System for Gravity Probe B, p. 64, Ph.D. Dissertation, Stanford University, Stanford, CA (1990).

Bardas, D., *et al.*, Hardware Development for Gravity Probe-B, *Proc. of SPIE*, **619**, 29 (1986).

Bencze, W.J., Gyroscope Spin Axis Direction Control for the Gravity Probe B Satellite, Ph.D. Dissertation, Stanford University, Stanford, CA (1996).

Chandler, J.F., R.D. Reasenberg, I.I. Shapiro, Testing General Relativity with Lunar Laser Ranging, *Procedures of the Seventh Marcel Grossmann Meeting on General Relativity*, eds. R.T. Jantzen and G.M. Keiser, 1501-1504, World Scientific, Singapore (1996).

Everitt, C.W.F., *et al.*, Report on a Program to Develop a Gyro Test of General Relativity in a Satellite and Associated Control Technology, GP-B Internal Report, Stanford University, Stanford, CA (1980).

Everitt, C.W.F., The Stanford Relativity Gyroscope Experiment: History and Overview, *Near Zero*, eds. J.D. Fairbank, B.S. Deaver, C.W.F. Everitt and P.F. Michelson, 587-639, Freeman, New York (1988).

Gwo, D.-H., S. Wang, K.A. Bower, J.A. Lipa, The Gravity Probe B Star-Tracking Telescope, *Adv. Space Res.*, this issue (2003).

Haupt, G.T., Development and Experimental Verification of a Nonlinear Data Reduction Algorithm for the Gravity Probe B Relativity Mission, Ph.D. Dissertation, Stanford University, Stanford, CA (1996).

Keiser, G.M., General Relativity Experiments in Space, *Adv. Space Res.*, this issue (2003).

Lebach, D.E., *et al.*, Measurement of the Solar Gravitational Deflection of Radio Waves Using Very Long Baseline Interferometry, *Phys. Rev. Lett.*, **75**, 1439 (1995).

Lockhart, J.M., SQUID Readout and Ultra-Low Magnetic Fields for Gravity Probe B (GP-B), *Proc. of the SPIE*, **619**, 148 (1986).

Muhlfelder, B., J.M. Lockhart and G.M. Gutt, The Gravity Probe B Gyroscope Readout System, *Adv. Space Res.*, this issue (2003).

Pound, R.V., G.A. Rebka, Apparent Weight of Photons, *Phys. Rev.*, **170**, 337 (1960).

Pugh, G.E., WSEG Research Memorandum Number 11, Weapons Systems Evaluation Group, The Pentagon, Wash., D.C. (1959).

Ratner, M.I., I.I. Shapiro, private communication, Smithsonian Astrophysical Observatory, Cambridge, MA (1996).

Schiff, L.I., Possible New Experimental Test of the General Theory of Relativity, *Phys. Rev. Lett.*, **4**, 215 (1960).

Shapiro, I.I., The Viking Relativity Experiment, *J. Geophysical Research*, **82**, 4329 (1977).

Taber, M.A., *et al.*, Results from the First Integrated System Tests of the Gravity Probe B Experiment, *The First William M. Fairbank Meeting on Relativistic Gravitation Experiments in Space*, eds. M. Demianski and C.W.F. Everitt, 211-226, World Scientific, Singapore (1993).

Taber, M.A., D. Bardas, S. Buchman, D.B. DeBra, C.W.F. Everitt, *et al.*, Gravity Probe B Payload Verification and Test Program, *Adv. Space Res.*, this issue (2003).

Turneaure, J.P., *et al.*, The Gravity-Probe-B Relativity Gyroscope Experiment: Approach to a Flight Mission, *Proceedings of the Fourth Marcel Grossmann Meeting on General Relativity*, ed. R. Ruffini, 411-464, Elsevier Science Publishers (1986).

Vassar, R., Error Analysis for the Stanford Relativity Gyroscope Experiment, Ph.D. Dissertation, Stanford University, Stanford, CA (1982).

Vessot, R.F.C., M.W. Levine, A Test of the Equivalence Principle using a Space-Born Clock, *Gen. Rel. Grav.* **10**, 181 (1979).

Will, C.M., *Theory and Experiment in Gravitational Physics*, Cambridge University Press, Cambridge, U.K. (1993).

Zhou, P., *et al.*, Multilayer Films of TiC, Ti and Cu for the Gravity Probe B Relativity Mission Gyroscopes, *Surface & Coatings Technology*, **76-77**, 516 (1995).